Science of the Total Environment 826 (2022) 154043

Contents lists available at ScienceDirect

Science of the Total Environment

journal homepage: www.elsevier.com/locate/scitotenv

Herbal plants- and rice straw-derived biochars reduced metal mobilization in fishpond sediments and improved their potential as fertilizers

Sajid Mehmood [a,b,1], Waqas Ahmed [a,b,1], Juha M. Alatalo [c], Mohsin Mahmood [a,b], Muhammad Imtiaz [d], Allah Ditta [e], Esmat F. Ali [f], Hamada Abdelrahman [g], Michal Slaný [h,i], Vasileios Antoniadis [j], Jörg Rinklebe [k,l], Sabry M. Shaheen [k,m,n,*], Weidong Li [a,b,**]

[a] Key Laboratory of Agro-Forestry Environmental Processes and Ecological Regulation of Hainan Province, Hainan University, Haikou 570228, China
[b] College of Ecology and Environment, Hainan University, Haikou City 570100, China
[c] Environmental Science Center, Qatar University, Doha, Qatar
[d] Soil and Environmental Biotechnology Division, National Institute for Biotechnology and Genetic Engineering, Faisalabad, Pakistan
[e] Department of Environmental Sciences, Shaheed Benazir Bhutto University Sheringal, Dir (U), Khyber Pakhtunkhwa 18000, Pakistan
[f] Department of Biology, College of Science, Taif University, P.O. Box 11099, Taif 21944, Saudi Arabia
[g] Cairo University, Faculty of Agriculture, Soil Science Department, Giza 12613, Egypt
[h] Institute of Inorganic Chemistry, Slovak Academy of Sciences, Dúbravská cesta 9, 845 36 Bratislava, Slovakia
[i] Institute of Construction and Architecture, Slovak Academy of Sciences, Dúbravská cesta 9, 845 03 Bratislava, Slovakia
[j] Department of Agriculture Crop Production and Rural Environment, University of Thessaly, Greece
[k] University of Wuppertal, School of Architecture and Civil Engineering, Institute of Foundation Engineering, Water- and Waste-Management, Laboratory of Soil- and Groundwater-Management, Pauluskirchstraße 7, 42285 Wuppertal, Germany
[l] University of Sejong, Department of Environment, Energy and Geoinformatics, Guangjin-Gu, Seoul 05006, Republic of Korea
[m] King Abdulaziz University, Faculty of Meteorology, Environment, and Arid Land Agriculture, Department of Arid Land Agriculture, Jeddah 21589, Saudi Arabia
[n] University of Kafrelsheikh, Faculty of Agriculture, Department of Soil and Water Sciences, 33516 Kafr El-Sheikh, Egypt

HIGHLIGHTS

- Herbal plants and rice biochar (BC) improved the fishpond sediments (FPS) quality.
- All biochars immobilized Cr, Cu, Zn and reduced their solubility and leachability.
- All biochars improved the macronutrients and carbon content in FPS.
- *T. mongolicum* (TMBC) was more effective than *T. terrestris* and rice straw BC.
- The biochars, particularly TMBC improved the potential of FPS as fertilizers.

GRAPHICAL ABSTRACT

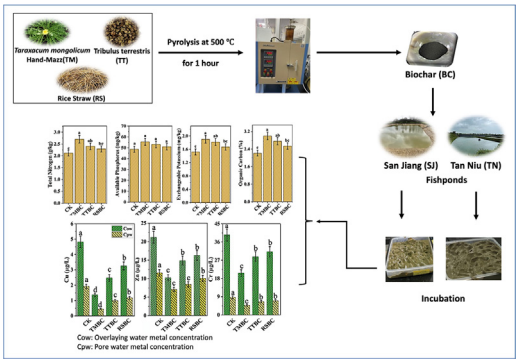

ARTICLE INFO

Article history:
Received 6 November 2021
Received in revised form 16 February 2022
Accepted 16 February 2022
Available online 21 February 2022

ABSTRACT

Fishpond sediments are rich in organic carbon and nutrients; thus, they can be used as potential fertilizers and soil conditioners. However, sediments can be contaminated with toxic elements (TEs), which have to be immobilized to allow sediment reutilization. Addition of biochars (BCs) to contaminated sediments may enhance their nutrient content and stabilize TEs, which valorize its reutilization. Consequently, this study evaluated the performance of BCs derived from

* Correspondence to: S.M. Shaheen, University of Wuppertal, School of Architecture and Civil Engineering, Institute of Foundation Engineering, Water- and Waste-Management, Laboratory of Soil- and Groundwater-Management, Pauluskirchstraße 7, 42285 Wuppertal, Germany.
** Correspondence to: W. Li, Key Laboratory of Agro-Forestry Environmental Processes and Ecological Regulation of Hainan Province, Hainan University, Haikou 570228, China.
E-mail addresses: shaheen@uni-wuppertal.de (S.M. Shaheen), 994362@hainanu.edu.cn (W. Li).
[1] These authors contributed equally to the work.

http://dx.doi.org/10.1016/j.scitotenv.2022.154043

Editor: Daniel CW Tsang

Keywords:
Fishpond sediments
Heavy metals
Immobilization
Biochar
Nutrients content

Taraxacum mongolicum Hand-Mazz (TMBC), *Tribulus terrestris* (TTBC), and rice straw (RSBC) for Cu, Cr, and Zn stabilization and for the enhancement of nutrient content in the fishpond sediments from San Jiang (SJ) and Tan Niu (TN), China. All BCs, particularly TMBC, reduced significantly the average concentrations of Cr, Cu, and Zn in the overlying water (up to 51% for Cr, 71% for Cu, and 68% for Zn) and in the sediments pore water (up to 77% for Cr, 76% for Cu, and 50% for Zn), and also reduced metal leachability (up to 47% for Cr, 60% for Cu, and 62% for Zn), as compared to the control. The acid soluble fraction accounted for the highest portion of the total content of Cr (43–44%), Cu (38–43%), and Zn (42–45%), followed by the reducible, oxidizable, and the residual fraction; this indicates the high potential risk. As compared with the control, TMBC was more effective in reducing the average concentrations of the acid soluble Cr (15–22%), Cu (35–53%), and Zn (21–39%). Added BCs altered the metals acid soluble fraction by shifting it to the oxidizable and residual fractions. Moreover, TMBC improved the macronutrient status in both sediments. This work provides a pathway for TEs remediation of sediments and gives novel insights into the utilization of BC-treated fishpond sediments as fertilizers for crop production.

1. Introduction

The persistence, toxicity, and bioaccumulation of heavy metals (HMs) in aquatic systems pose a serious threat to human health, and result in adverse environmental impacts (Shaheen et al., 2020; Alamri et al., 2021; Kong et al., 2021). With the progress humankind has made with the industrial processes, HMs levels have increased from a few milligrams to several hundred milligrams per kilogram of the containing medium, e.g., in the riverine systems (Wang et al., 2020; Rinklebe et al., 2019) in the vicinity of mining sites and smelting areas, posing serious hazards to ecosystems and human health (Lin et al., 2019; Khan et al., 2021). Most of the living organisms, plants and microorganisms, deteriorate dramatically when found under stress related to HMs-induced toxicity (She et al., 2021).

Copper (Cu), zinc (Zn), and chromium (Cr) are released into sediments through mining, fish farming, shipping activities, pesticides, fossil fuel combustion, tourism, and natural continuous inputs (Chang et al., 2021; Khan et al., 2021; Ota et al., 2021). When entering water systems, HMs are usually sorbed onto, or occluded into, solid particles (suspended solids and sediments); thus, their concentrations are usually higher in sediments than those dissolved in water (Wang et al., 2019). Although HMs, when sorbed onto the surface of sediments, exhibit a low toxicity risk (Yang et al., 2021), changes in sediment pH, specific surface area, and nutrients content can alter the sediment retention capacity and consequently the sorption of HMs (Kong et al., 2021; Miranda et al., 2021; Zhang et al., 2020).

Fishpond sediments are rich in nutrients and organic matter, and could, thus, be a valuable fertilizer for crop production (Shaheen et al., 2020). Accumulation of nutrients in sediments has been widely described in the literature (Han et al., 2020; Haque et al., 2016; Kong et al., 2021; Ouyang et al., 2021; Wiener et al., 2020; Zhang et al., 2020); however, the persistence of HMs on sediment particle surfaces makes the recovered sediments unsuitable for direct application (Haque et al., 2016). Therefore, HMs stabilization in sediments and their transformation into environment-friendly amendments is needed to enable their safe use as fertilizers in agriculture (Palansooriya et al., 2020).

The fractionation of HMs in sediments in various pools includes: (a) the acid-soluble, (b) reducible, (c) oxidizable, and (d) residual fraction, where the HMs mobility and bioavailability gradually decrease from the acid-soluble to the residual fractions. The basic principle of soil/sediment remediation is to shift the existing HMs from the mobile and active forms towards the immobile/residual fractions, so that their bioavailability may be reduced (Palansooriya et al., 2020; Zhang et al., 2020). The immobilization techniques of HMs can effectively mitigate the mobility of HMs (Beiyuan et al., 2018; Khan et al., 2021; Ali et al., 2022). Numerous studies on sediment treatments have shown the advantages of using carbonaceous materials to immobilize HMs (Miranda et al., 2021; Shaheen et al., 2020; Yang et al., 2021). Among those tested, biochar (BC) has received great attention for remediation of HMs contaminated soils, sediments, and water due to its low cost, relatively high abundance, high sorption capacity, environment friendly composition (Ali et al., 2020; El-Naggar et al., 2021; Shaheen et al., 2022a, 2022b; Wen et al., 2021), as well as its high surface area and abundant reactive surface functional groups (Bolan et al., 2022; Shaheen et al., 2022a).

Biochar has been used as soil amendment, immobilizing agent, and nutrient carrier in soil and water (El-Naggar et al., 2019; Bolan et al., 2022; Farid et al., 2022; Shaheen et al., 2022a) and has been reported to exhibit unique advantages in removing or fixing HMs, in in-situ sediment/soil remediation (Palansooriya et al., 2020; Kong et al., 2021; Azeem et al., 2022). However, BC physical and chemical properties depend on the pyrolysis conditions and feedstock characteristics (Fu et al., 2021; Shaheen et al., 2019, 2022a; Sial et al., 2022). Generally, higher pyrolysis temperature leads to larger surface area (Guo et al., 2020), but the structural characteristics of the produced BC are dependent on the composition and quantity of (in)organic compounds in the feedstock (Chen et al., 2020). In fact, the raw materials have a greater influence, than the pyrolysis temperature, on the concentration and composition of HMs in BCs (Qiu et al., 2015; Farid et al., 2022). Previous works showed that BC from high temperature pyrolysis mixed with HM-contaminated sediments was more effective in reducing the mobility, toxicity, and bioavailability of contaminant HMs (Kong et al., 2021; Liu et al., 2018; Lou et al., 2012).

The efficiency of BCs for HMs immobilization in soils has been extensively studied during the last decade; however, limited studies have documented the production of biochar from non-contaminated residues of herbal plants to stabilize HMs in contaminated sediments for the valorization and improvement of the sediments potential as fertilizers. The novelty of this work lies in the valorization of available wastes, providing detailed characterization of biochar from newly used feedstock and in the transformation of fishpond sediments into an acceptable soil amendment and fertilizer. With the increased prices and demand in conventional fertilizers and with the parallel increase in soil contamination, biochar and fishpond sediment mixtures shall provide environmental, economic and human health solutions for the agricultural production in contaminated soils, especially in low-income countries. The overall objective of this work was to produce BCs from *Taraxacum mongolicum* Hand-Mazz (Mongolian dandelion), *Tribulus terrestris* (puncture vine), and *Oryza sativa* (rice) straw and use it to immobilize HMs in contaminated sediments in an effort to render the sediments suitable for use as fertilizers in crop production. Thus, this study investigated, in a laboratory scale, the effect of these BCs on the removal/immobilization of Cu, Zn, and Cr, from two different fishpond sediments to assess their fertilization potential, and consequent improvement of the treated sediments. Specifically, the study aims were to: (i) produce three different BCs from locally available residues and provide information on their characteristics and suitability for HM immobilization in sediments; and (ii) identify the possible mechanism(s) of HM immobilization through the use of Spearman correlation coefficient and the significance of various factors, including BC physicochemical characteristics, sediment characteristics, HMs concentrations in the water phase, toxicity characteristic leaching procedure (TCLP), and the speciation of HMs in sediments.

2. Materials and methods

2.1. Study area and sediment collection and characterization

Sediments were collected from fishponds located in San Jiang (SJ) and Tan Niu (TN) in eastern Hainan Province, China (Supplementary Materials;

Fig. S1). The sediment samples were obtained in June 2020: sampling was performed at five parallel points using a core sampler at both sites. The sediment subsamples were mixed to obtain composite samples, air-dried (~25 °C), and then passed through a sieve to obtain fully homogenous sediment. All sediment samples were stored in air-tight plastic bags until subsequent analyses. Chemical and nutrient analyses of the collected TN and SJ sediments were performed following the methods explained in detail in Section 2.5. Basic attributes of the sediments and BCs are presented in Table 1.

2.2. Biochar production and characterization

Raw materials of *Taraxacum mongolicum* Hand-Mazz, *Tribulus terrestris*, and rice straw were collected from Xiuying District, Haikou City, Hainan Province, China, and used in this study to produce BCs, as they were reported to be effective against HMs in trials reported elsewhere (Ahmed et al., 2021a, 2021b, 2021c, 2021d, 2021e). The collected plant materials were washed with ultrapure water (18.2 MΩ cm^{-1} at 25 °C) to remove impurities and then dried and pyrolyzed using a tube furnace (OTF-1200×, Hefei Kejing Materials Technology Co., Ltd., China). The tube furnace was heated at temperature that increased at a rate of 7 °C min^{-1} until it reached 500 °C, which was maintained for 1 h. Then, the tube furnace was cooled to room temperature and the BCs were collected and labeled: TMBC (*T. mongolicum* Hand-Mazz-derived BC), TTBC (*T. terrestris*-derived BC), and RSBC (rice straw-derived BC). The charred materials were then stored in air-tight bags for subsequent use and analyses.

The surface morphology of biochars (BCs) was studied by using Scanning Electron Microscope (SEM; TM3000, Hitachi, Japan) at an accelerated voltage of 5–10 kV. The quality, shape, and size of BCs were examined by Transmission Electron Microscope (TEM; FEI Tecnai S-TWIN, USA) at an accelerated voltage of 100 kV. An elemental analyzer (Vario EL Cube, Elementar, Germany) was used to evaluate the BCs elemental concentrations. Biochar specific surface area (SSA) was determined using an automatic specific surface and aperture distribution analyzer (Autosorb-IQ, Quanta chrome, USA). Before each measurement, all samples were degassed in the apparatus for 1 h at 500 °C. The specific surface area calculation was based on the Brunauer Emmett Teller (BET) formalism. Fourier transform infrared (FTIR) spectra of BCs were obtained by a Nicolet (5700, USA) spectrometer. The BCs were ground to powder, 1 mg of sample was mixed with 200 mg KBr. Subsequently infrared (IR) spectra were recorded in the range of 4000–400 cm^{-1} with 64 scans at resolution 4 cm^{-1}. The X-ray diffraction (XRD) patterns of the produced BCs were examined by X-ray diffraction analysis carried out in a Bruker D8-Advance X-ray diffractometer (Bruker, Germany) using CuKα (λ = 0.154 nm) radiation at a scanning rate of 1° min^{-1} with an angle ranging from 2° to 50° of 2θ. The composition of BC samples and their valence states were examined via X-ray photoelectron spectroscopy (XPS) using the ESCALAB 250Xi XPS X-ray photoelectron spectrometer (Thermo Fisher Scientific, USA).

Table 1
Basic properties and elements content in the studied sediments and biochars.

Parameter	Unit	Sediments		TMBC	TTBC	RSBC
		TN	SJ			
pH	–	6.06	7.92	8.91	8.69	8.55
EC	dS/m	1.45	1.28	0.60	0.57	0.31
Total N	g/kg	1.59	2.11	1.98	1.110	0.650
Available P	mg/kg	200	48.80	197.4	150.5	141.7
Exchangeable K	g/kg	1.28	1.54	1.97	1.60	1.35
Total Ca	g/kg	1.6	11.40	2.51	1.48	0.17
Total Mg	g/kg	2.1	4.10	0.41	0.32	0.17
Total Na	g/kg	1.3	5.90	0.16	0.32	0.11
Organic C	%	1.32	2.34	77.09	52.06	37.35
Surface area	$m^2\ g^{-1}$	–	–	3.12	1.84	0.84
Particle size						
2.0–0.05 mm	g/kg	384	472	–	–	–
0.05–0.002 mm	g/kg	380	439	–	–	–
<0.002 mm	g/kg	236	89	–	–	–
Total Cu	mg/kg	18	9	2.2	1.59	5.9
Total Zn	mg/kg	28	40	7.0	18.0	4.7
Total Cr	mg/kg	38	53	n.d.	0.10	2.3

TMCC = *Taraxacum mongolicum* Hand- Mazz-derived biochar.
TTBC = *Tribulus terrestris*-derived biochar.
RSBC = rice straw-derived biochar.
TN: Tan Niu fishpond sediments.
SJ: San Jiang fishpond sediments.
n.d.: not detected.

2.3. Sediments treatment with biochar

A sample of each sediment (100 g dry weight) was mixed with 120 mL of ultrapure water (18.2 MΩ cm^{-1} at 25 °C), in triplicate, and allowed to stand for 24 h in a 250 mL screw-mouth bottle (Wang et al., 2019). Then, 3 g of each of the BCs were added to the bottle, in triplicate for TN and SJ sediments. A treatment consisting of bottles containing only sediment without BC was regarded as control (CK). After sealing, the bottles were shaken intensively to ensure thorough mixing of the BC and the sediment, and the mixture was then kept in an incubator for 90 days at constant temperature (20 ± 1 °C) in the absence of light to allow the contents to interact naturally.

2.4. Metal extraction and analyses

2.4.1. Metal in overlying water and pore water

After incubation, the overlying water was completely withdrawn and passed through a 0.45-μm filter before analysis. The remaining sediment-BC mixture was centrifuged at 4000 rpm for 15 min for further water separation from the pores, and then the pore water extracted was also 0.45-μm filtered. Similar techniques have been used and reported in Tou et al. (2021). Concentrations of Cr, Cu, and Zn in the overlying water (C_{ow}) and pore water (C_{pw}) were analyzed by inductively-coupled plasma optical emission spectrometry (ICP-OES; Optima 8000).

2.4.2. Metal fractionation in sediments

The geochemical fractions of Cr, Cu, and Zn in the TN and SJ sediments were extracted sequentially using the method of the Commission of the European Communities Bureau of Reference (BCR; Ure, 1991; Ure et al., 1993; Rauret et al., 1999), which is also used by Jiang et al. (2012), Rinklebe and Shaheen (2017), and Shaheen et al. (2017). The metals were fractionated sequentially to four operationally defined fractions as follows: F1: acid-soluble; F2: reducible; F3: oxidizable; and F4: residual (Supplementary Materials; Table S1). The extracted metal fractions were analyzed using the ICP-OES (Optima 8000).

2.4.3. Toxicity characteristic leaching procedure (TCLP)

The leaching potential of the HMs in the TN and SJ sediments was measured using the TCLP method 1311, developed by the U.S. Environmental Protection Agency. An extracting solution was prepared using glacial acetic acid (CH_3COOH; pH = 4.93 ± 0.05; USEPA, 1991). Forty mL of the extracting solution and 2 g of sediment were mixed and stirred at 190 rpm for 18 h (25 °C), and then centrifuged at 4000 rpm for 15 min. The supernatant was passed through a 0.45-μm filter, and the concentrations of Cr, Cu, and Zn were finally analyzed using the ICP-OES (Optima 8000).

2.5. Characterization and nutrients content in the sediments

Both, finely ground, sediments were characterized by following the standard methods described in Page (1982). The pH was measured by the potentiometric method with the pH meter HJ 962-2018. The sediments electrical conductivity (EC) was measured by the electrode method (HJ 802-2016). Total nitrogen was determined by the wet oxidation and micro-Kjeldahl method (LY/T 1228-2015). Available P and exchangeable K were determined by extraction with sodium bicarbonate (NY/T 1121.7-2014), and ammonium acetate (LY/T 1246-1999), respectively. Total Ca,

Mg and Na in both sediments were determined by following the "NY/T 296-1995" method and then the contents of Ca and Mg were analyzed on an atomic absorption spectrophotometer, while the Na content was measured on a flame photometer. Carbon content was detected by a general detection method for chemical characteristics of domestic waste (CJ/T 96-2013) and analyzed by the elemental analyzer. The hydrometer method was used to determine the sediment particle distribution (LY/T 1225-1999). The total content of Cu, Zn, and Cr in both sediments was extracted and measured by ICP-OES (Optima 8000). Basic properties, metal and nutrients content in the sediments and BCs are presented in Table 1.

2.6. Data quality assurance and statistical analysis

All treatments and experiments were performed in triplicates. Quality control of the extraction efficiency of the metal concentrations was performed using certified reference samples. The average recovery percentages were 99.6% for Cr, 96.6% for Zn and 103.7% for Cu. Also, blank and triplicate measurements were employed for analyses. Standard solutions (Merck) were routinely used to guarantee high quality results. The maximum relative standard deviation (RSD) between replicates was set to 10%. To verify the quality of the fractionation data, we compared the fractions summation of each metal with the metal total content, and found that the recovery percentage ranged between 90 and 112%. The statistical analyses were carried out using IBM SPSS Statistics 23 (NY, USA). The means for the variables were tested using one-way ANOVA with Duncan's multiple range tests at a significance level of $p < 0.05$. OriginPro 9.1 b215 (OriginLab Corporation, Northampton, USA) was used to create the figures. The "*heatmap*" package in the R software was used as per Jia et al. (2017).

3. Results and discussion

3.1. Characterization of biochars

The biochar characterization techniques can depict the structure, surface functional groups and elemental analysis (Brewer et al., 2014). The SEM and TEM images of the BCs derived from the different raw materials

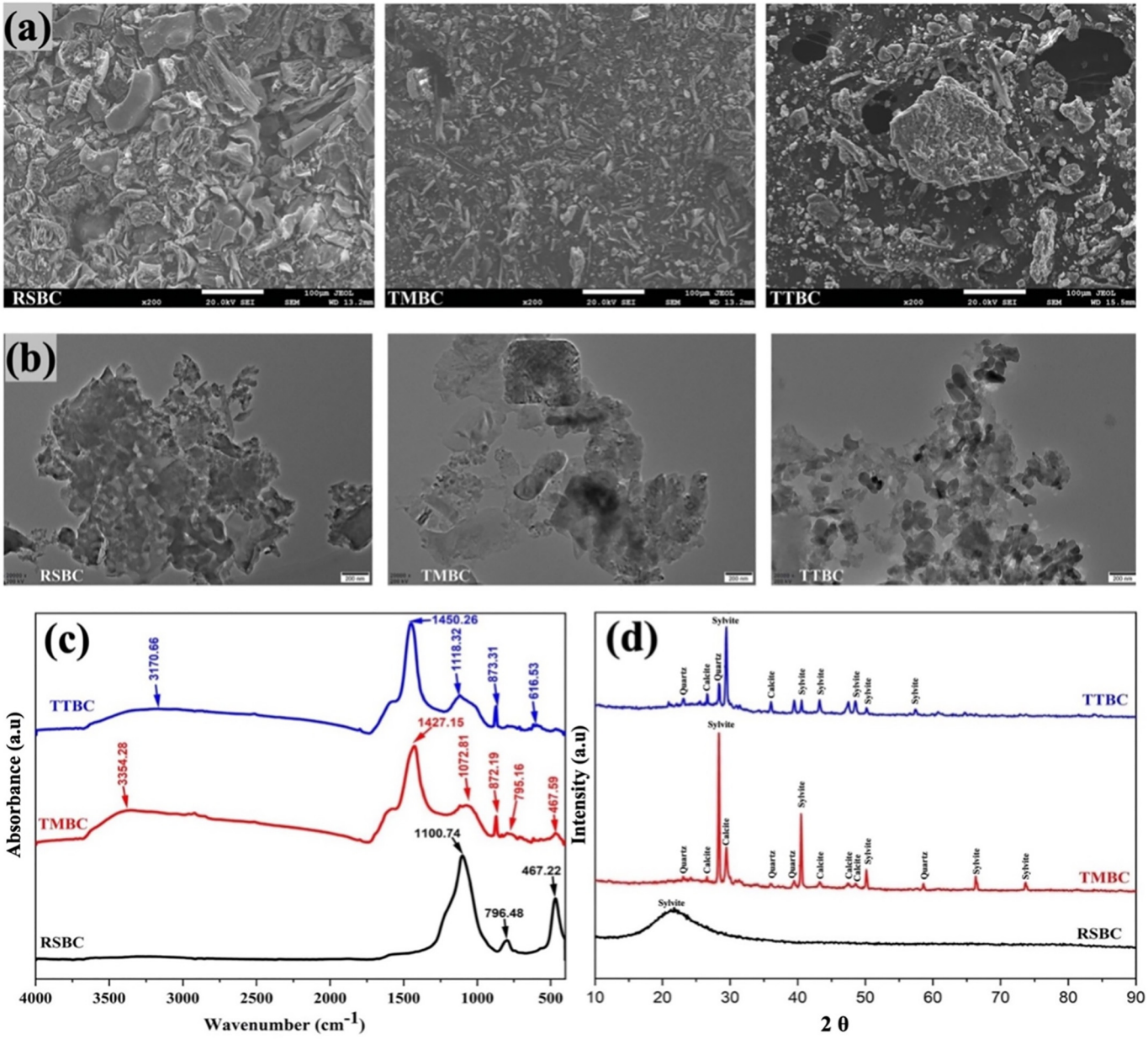

Fig. 1. (a) Scanning electron microscope (SEM) images, (b) transmission electron microscopy (TEM) images, (c) Fourier transform infrared (FTIR) spectra, and (d) X-ray diffraction (XRD) spectra of *Taraxacum mongolicum* Hand-Mazz-derived biochar (TMBC), *Tribulus terrestris*-derived biochar (TTBC), and rice straw-derived biochar (RSBC).

are shown in Fig. 1 and revealed their microstructures and surface morphology. As shown in Fig. 1A, RSBC and TMBC had irregular morphological structures, which is consistent with other findings (Ahmed et al., 2021a, 2021b, 2021c, 2021d, 2021e), whereas the TTBC structure was relatively granular with vascular bundle structures. The TEM analysis (Fig. 1B) shows that the number of mesoporous structures increased due to pyrolysis. Further findings revealed a uniform layered structure of RSBC, TMBC, and TTBC (Fig. 1B), confirming their high-impact utilization in environmental engineering.

The FTIR spectra of TMBC and TTBC revealed that these BCs contained almost identical functional groups, except for the absorption bands at lower wavenumber than 1400 cm^{-1}. The infrared spectrum of RSBC was completely different compared to its counterparts (Fig. 1C). The reactive groups on all BCs surfaces were represented by the following absorption bands: OH stretching of Hbonded hydroxyl groups at 3354 cm^{-1}, CC stretching, indicative of lignin and aromatic C at 1450 cm^{-1}, a band approximately at 1427 cm^{-1} represents the OH stretches of carboxylic groups in BC. Aromatic (CO) and phenol (OH) at 1265 cm^{-1}, COC symmetric stretching in ester groups of cellulose and hemicellulose at 1106 cm^{-1}, (OH) at 998 cm^{-1}, and aromatic (CH) at 829 cm^{-1} were also observed (Mossop and Davidson, 2003; Jia et al., 2017; Slaný et al., 2019; Kumar et al., 2020; Slaný et al., 2022). However, the intensities of these absorption bands varied with different raw material, indicating a variation in the amount of these reactive groups. For example, the TMBC exhibited higher stretching vibration absorption intensities compared with the RSBC and TTBC, implying additional oxygen-containing functional groups such as those at 3170 cm^{-1} (OH), at 1450 cm^{-1} (CO), and at 873 cm^{-1} (OH). The main factors that influence BC surface functional groups are feedstock and pyrolysis temperature (Li et al., 2017). In addition, changes in feedstock properties such as an increased pH, surface area and/or porosity can reduce BC functional groups (Yaashikaa et al., 2020). Therefore, at the specific pyrolysis temperature applied, the raw materials used for BC production can be considered as the main factor determining the surface chemical properties of the produced BCs. In addition, the diversity of absorption functional groups in BCs makes form them high quality adsorbents.

The structural mineralogy of all BCs was assessed based on the XRD patterns (Fig. 1D), a high quality, fast and non-destructive analysis (Yaashikaa et al., 2020). Different mineral crystals were found in BCs, including mainly quartz, sylvite, and calcite (Singh et al., 2010). These minerals are generally known to be very good adsorbents. In TTBC and TMBC, this diverse representation of diffraction peaks is evident compared to RSBC, which also correlates well with FTIR results. The TMBC showed higher BET surface area (3.12 $m^2\ g^{-1}$; Table 1) than TTBC (1.84 $m^2\ g^{-1}$) or RSBC (0.84 $m^2\ g^{-1}$), which could be due to the release of volatile substances and the development of a vascular bundle structure after pyrolysis (Kim et al., 2013). Higher surface area of a BC favors HMs adsorption on its surface (Zhang et al., 2020); therefore, selection of appropriate BC is a key factor for effective site restoration.

The chemical composite and structure of BCs were further determined by XPS (Fig. 2). X-ray photoelectron spectroscopy (XPS) is very useful and a surface-sensitive quantitative spectroscopic technique based on the photoelectric effect that can identify the elements that exist also within a biochar or are covering its surface. The XPS spectra of the TTBC and RSBC samples showed similar characteristic peaks assigned to C 1s, and O 1s, while the Ca 2p peak only appeared in the TMBC sample. We further infer the mechanisms from the C 1s (Fig. 2A) and O 1s (Fig. 2B) spectra. The three peaks at C1s were contributed from the CC/H, COC/H, and OCO at 284.5 eV, 285 eV, and 286 eV, respectively, which is similar to the result of biochar's C 1s deconvolutions from other studies (Ahmed et al., 2021e; Reguyal and Sarmah, 2018). The O 1s spectra can be separated into three peaks, which can be observed at 530 eV, 531.3 eV and at 532.4 eV. Data about content of functional groups in BCs from XPS spectroscopy correlated well with the FTIR and XRD results. This finding also proves that these materials can adsorb heavy metals very well also due to the content of strong adsorption groups. The valencies of Cr 2p were separated at 577.93 eV (Cr $2p_{1/2}$) and 588.0 eV (Cr $2p_{3/2}$) (Liang et al., 2020). This finding is most visible in the case of the TMBC sample. During the adsorption process, consequently, some Cr was adsorbed onto the surface of BCs as well. Further, BC spectra show a new peak at 285 eV corresponding to the CC coordination, due to the fact that equilibration with Cr resulted in major changes on the BCs surface. To further characterize the mechanism of Cu sorption on BCs, the changes in the constituent elements of BCs, after the adsorption of Cu were also analyzed. The C 1s spectrum of BCs consisted of two fitted peaks, including CC and OCO, and was centered at binding energies of 284.8 eV and 285.64 eV, respectively. These peaks indicated the successful carboxylation of the biochars. In XPS investigation, since carbon, nitrogen, sulfur and oxygen can change the reactivity of biochar surfaces, their high resolution spectra are significant for the elucidation of the adsorption mechanisms. High resolution of the C 1s spectra of both control and Zn-laden biochar samples created peaks that appeared at 283.57 eV and 284.21 eV, respectively; these can be attributed to the alpha-carbon, hydrocarbon chains (C_xH_y) CS, CN and carboxylic and hydroxyl groups present as organic functional groups on cellulose, lignin, other polysaccharides and proteins of the biochar. The deconvolution of O 1s spectra of the control and Zn-laden biochar comprises of peaks with binding energy of 531.95 eV, 532.08 eV and 532.42 eV, which represented the functional groups of CO, CO, OCO and phosphates (Ramrakhian et al., 2022). XPS confirmed that surfaces of biochars were significantly involved in the binding with Cr, Cu and Zn.

3.2. Effect of biochars on sediment properties and nutrients content

The chemical and nutrients analyses of the two fishpond sediments confirmed that there were high levels of nutrients present in the sediments, qualifying their potential use as fertilizers. However, the mean pH values of the unamended sediments were substantially different (SJ pH = 7.92; TN pH = 6.06). Biochar addition increased the pH of both sediments; however, the increase was non-significant. Higher pH values were recorded in sediments treated with TMBC; the pH increased to 8.1 and 6.18 for SJ and TN sediments, respectively (Table 2). The high pH of the TN sediment could potentially restrict the growth of some crops; however, the pH of SJ was more favorable for plant growth (5.0–7.0) where plant nutrients availability and microbial activities are beneficial (Kallenbach et al., 1996). A similar trend was noted in terms of the electrical conductivity (EC) in both sediments: TMBC addition increased sediments EC from 1.28 dS m^{-1} to 1.47 dS m^{-1} at SJ and from 1.45 dS m^{-1} to 1.66 mS cm^{-1} in the TN sediment.

The plant nutritional value of both sediments was significantly improved when BCs were incorporated, caused by the added nutrients and adsorbed HMs from the sediments due to their chemical reactivity (Ghosh et al., 2011; Farid et al., 2022). The addition of TMBC to the SJ sediment substantially increased total nitrogen (N) by 28.0%, available phosphorus (P) by 14.0%, and exchangeable potassium (K) by 25.0%, as compared to the control (Fig. 3). The addition of TMBC to the TN sediment increased total N by 31.0%, available P by 14.5%, while it decreased exchangeable K by 71.0%, as compared to the control (Fig. 3). A similar trend was observed for calcium (Ca) and magnesium (Mg) following TMBC incorporation, with increases of 21.1% (Ca) and 17.4% (Mg) in the SJ sediment and 20.6% (Ca) and 17.1% (Mg) in the TN sediment. These observations confirm previous findings that incorporating BCs in a contaminated environment increases plant nutrients and helps alleviate plant tolerance for HMs, which is necessary for sustainable plant production (Hagemann et al., 2017; Hossain et al., 2020; Farid et al., 2022). Organic carbon (OC) content was also significantly ($P \leq 0.05$) increased after BCs addition. For example, TMBC incorporation increased OC by ca. 36% and 32% in the SJ and TN sediments, respectively (Fig. 3). As the plant nutrients content in SJ and TN sediments were *quasi* identical, adding BC improved their fertilization potential in the order of TMBC>TTBC>RSBC, which shows that TMBC was the most effective in improving sediment nutrients level (Table 2; Fig. 3).

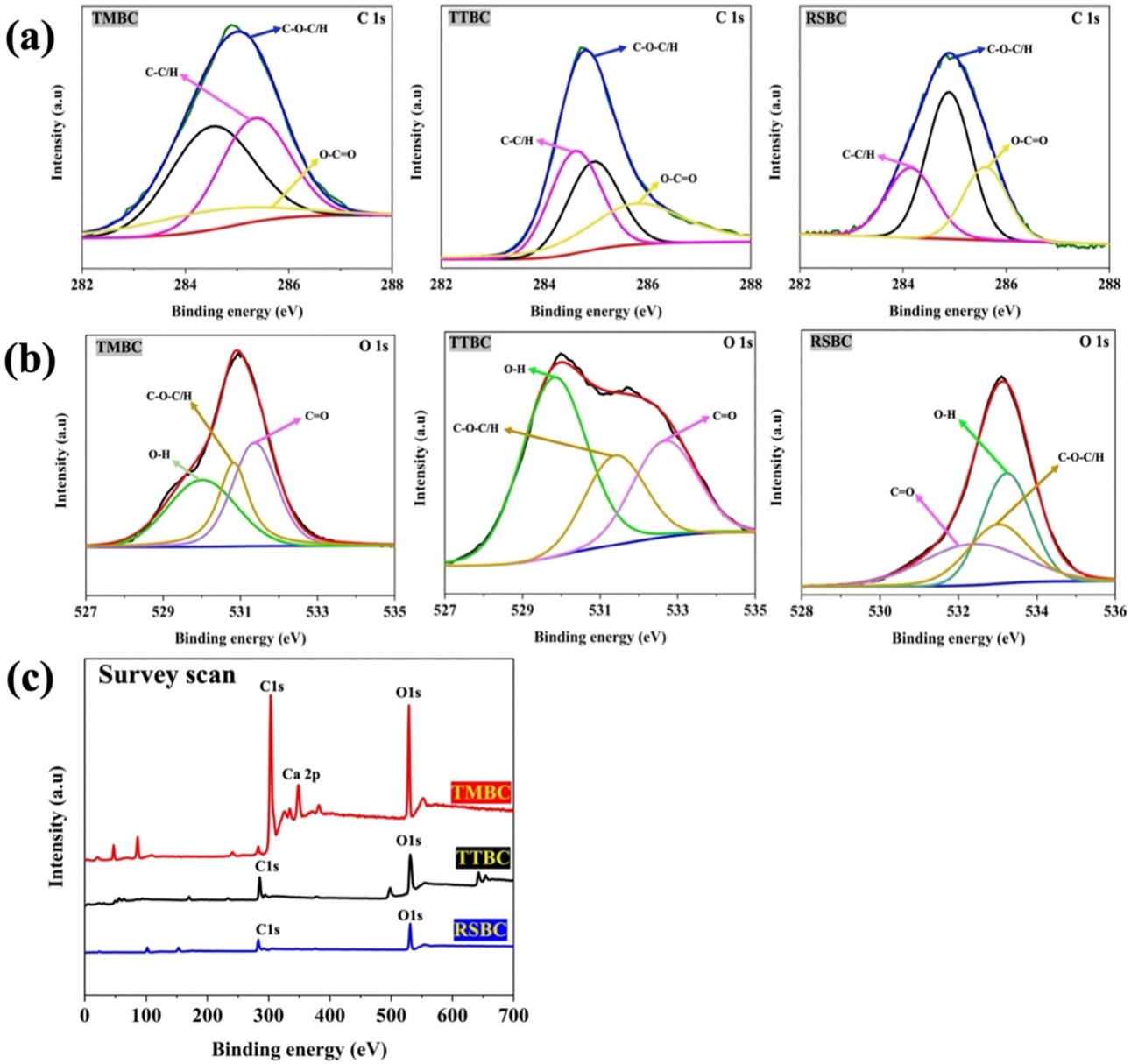

Fig. 2. C1s (A), O1s (B) spectra and survey scans (C) of *Taraxacum mongolicum* Hand-Maz biochar (TMBC), *Tribulus terrestris* biochar (TTBC), and rice straw biochar (RSBC).

3.3. Effect of biochars on dissolved metal concentrations

The ecological risk induced by HMs on water bodies has been thoroughly studied (Kong et al., 2021; Ota et al., 2021). In aquatic ecosystems, dissolved metal concentrations is more relevant than that concentrations in sediments as the dissolved fraction has an immediate effect and can be regarded as toxicity predictors (Tang et al., 2016). The average concentrations of Cr, Cu, and Zn in the overlying water (C_{ow}, μg L^{-1}) were 39.5, 4.8, and 21.2 in the untreated SJ sediments, and 26.0, 11.5, and 17.3 in the untreated TN sediments, respectively (Fig. 4). Biochar addition significantly reduced metals concentrations in the C_{ow} (Fig. 4). As compared with the unamended sediments (control), TMBC was more effective in reducing the average concentrations (μg L^{-1}) of Cr (by 47% in SJ and 51% in TN), Cu (by 71% in SJ and 52% in TN), and Zn (by 51% in SJ and 68% in TN) in the C_{ow} of both sediments than was the TTBC (by 27–29% for Cr, by 20–48% for Cu, and by 29–36% for Zn) and RSBC (by 27–29% for Cr, by 20–48% for Cu, and by 29–36% for Zn; Fig. 4).

The average concentrations of metals in the sediments pore water (C_{pw}, μg L^{-1}) were 6.7 for Cr, 1.9 for Cu, and 11.5 for Zn in the untreated SJ sediment, while they were 8.7 for Cr, 3.8 for Cu, and 7.7 for Zn in the untreated TN sediment (Fig. 4). Biochar addition significantly reduced the metals concentrations also in the C_{pw} (Fig. 4). As compared with the unamended sediments (control), TMBC was more effective in reducing the average concentrations (μg L^{-1}) of Cr (by 77% in SJ and 45% in TN), Cu (by 76% in SJ and 71% in TN), and Zn (by 38% in SJ and 50% in TN) in the C_{pw} of both sediments than was TTBC (24–34% for Cr, 47–48% for Cu, and 16–26% for Zn) and RSBC (19–25% for Cr, 28–38% for Cu, and 5–12% for Zn) (Fig. 4). These results indicate that the metal concentration in the C_{ow} of all treatments was higher than C_{pw}, which might be explained by the metals release from sediments to the C_{ow} during the 90 days incubation period under the flooded conditions. We assume that flooding the sediments may have reduced the redox potential (Eh), which caused a reductive dissolution of the Fe-Mn oxides and microbial decomposition of organic matter, and subsequently release of the associated metals to the C_{ow}. This interpretation concurs with recent findings reported elsewhere (e.g., El-

Table 2
Changes in quality parameters of the San Jiang and Tan Niu fishpond sediments following addition of the studied biochars. Results are mean values ± standard deviation (n = 3). Different small letters indicate significant differences at $P < 0.05$.

Parameter	Units	CK	TMBC	TTBC	RSBC
San Jiang fishpond sediment					
pH		7.92 ± 0.46a	8.1 ± 0.54a	8.17 ± 0.51a	8.08 ± 0.49a
EC	dS/m	1.28 ± 0.07a	1.47 ± 0.09a	1.41 ± 0.08a	1.34 ± 0.08a
Total element content					
Ca	g/kg	11.1 ± 0.66b	13.8 ± 0.80a	12.950 ± 0.7ab	12.150 ± 0.71ab
Mg	g/kg	3.8 ± 0.23b	4.8 ± 0.28a	4.562 ± 0.26a	4.325 ± 0.25ab
Na	g/kg	5.5 ± 0.34b	6.9 ± 0.40a	6.610 ± 0.38a	6.245 ± 0.37ab
Cu	mg/kg	8.7 ± 0.53a	6.54 ± 0.38b	7.621 ± 0.44ab	8.282 ± 0.48a
Zn	mg/kg	39.8 ± 2.34a	30.3 ± 1.77c	33.288 ± 1.9bc	36.490 ± 2.14ab
Cr	mg/kg	51.5 ± 3.10a	40.2 ± 2.35c	44.107 ± 2.5ab	48.349 ± 2.83bc
Tan Niu fishpond sediment					
pH		6.06 ± 0.35a	6.19 ± 0.42a	6.59 ± 0.40a	6.42 ± 0.38a
EC	dS/m	1.45 ± 0.09a	1.66 ± 0.10a	1.560 ± 0.09a	1.52 ± 0.09a
Total element content					
Ca	g/kg	1.52 ± 0.09a	1.937 ± 0.11b	1.818 ± 0.11b	1.705 ± 0.100b
Mg	g/kg	1.97 ± 0.12b	2.465 ± 0.14a	2.337 ± 0.14a	2.215 ± 0.130ab
Na	g/kg	1.1 ± 0.08b	1.542 ± 0.09a	1.457 ± 0.09a	1.376 ± 0.080a
Cu	mg/kg	17.6 ± 1.05a	14.027 ± 0.82b	15.243 ± 0.89ab	16.564 ± 0.97a
Zn	mg/kg	27.5 ± 1.64a	21.257 ± 1.24c	23.302 ± 1.36bc	25.543 ± 1.49ab
Cr	mg/kg	37.7 ± 2.22a	28.849 ± 1.69c	31.624 ± 1.85bc	34.666 ± 2.09ab

TMCC = *Taraxacum mongolicum* Hand- Mazz-derived biochar.
TTBC = *Tribulus terrestris*-derived biochar.
RSBC = rice straw-derived biochar.

Naggar et al., 2018; Rinklebe et al., 2016; Shaheen and Rinklebe, 2017; Shaheen et al., 2014, 2017, 2020; Yang et al., 2021) where HMs concentration increased due to the reductive dissolution.

The concentrations of Cr in the C_{ow} were higher than Cu and Zn (Fig. 4), which might be due to the higher total content of Cr than Cu and Zn (Table 1). Also, the precipitation of Cu and Zn, particularly of Cu, with sulfides under reduced conditions due to saturation could be a reason for their lower release as compared to Cr (Shaheen et al., 2017). Heatmap analyses (Fig. 5) further confirmed these results and showed a positive correlation between metals in the aqueous phase and sediments, which is in agreement with the findings of Cheng et al. (2015) and Shaheen et al. (2020).

The results (Fig. 4) also indicate that the three BCs reduced significantly the metals concentrations in the overlying and pore water, as compared to the unamended sediments. However, the efficiency of TMBC was substantially higher than that of TTBC and RSBC. Although TMBC was the most effective, the TTBC and RSBC could also adsorb metals on their surface and mitigate their release from sediment to the liquid phase, i.e., the C_{ow}. The higher efficacy of TMBC over TTBC and RSBC is linked with the higher surface active functional groups of TMBC (e.g., OH, CO, and OH), its higher crystallinity, and higher BET surface area (Table 1) compared to TTBC and RSBC (Fig. 1). Also, XPS data in Fig. 2 shows that the intensities of the peaks associated with oxygen groups in RSBC are slightly weaker than in the other two types of biochars (i.e., TMBC and TTBC) indicating that the oxygen functional groups of RSBC distributed in the inner sheet were difficult to reduce.

3.4. Effect of biochars on metals leachability

The average concentrations of TCLP-extracted Cr, Cu, and Zn (mg L^{-1}) were 2.06, 0.24, and 1.25 in the untreated SJ sediment, and 1.59, 0.72, and 1.06 in the untreated TN sediment, respectively (Fig. 6). Metal concentrations (mg/ kg) are presented in the supplementary materials (Fig. S2). Biochar addition notably reduced the TCLP-extracted Cr, Cu, and Zn as compared to the unamended sediments (Fig. 6). Also, TMBC was more effective, compared to the control, in reducing the average concentrations (μg L^{-1}) of Cr (by 47% in SJ and 45% in TN), Cu (by 60% in SJ and 37% in TN), and Zn (by 62% in SJ and 44% in TN) than was TTBC (32–33% for Cr, 4.0–40% for Cu, and 30–42% for Zn) or RSBC (16–20% for Cr, 2.0–20.0% for Cu, and 12–31% for Zn; Fig. 6). This observation confirms the effectiveness of the tested BCs for mitigating the solubility and leachability of Cr, Cu, and Zn in the studied sediments. However, although all BCs reduced the leachability of the three metals, TMBC exhibited a higher ability than the other two BCs (Fig. 6).

These results were further verified by the heatmap analysis, which provided indications of the relationship between HMs parameters and sediments (Fig. 5). The heatmap results revealed rather complex relationships between parameters and the sediments, i.e., a significant ($p < 0.05$) positive correlation between TCLP-extractable Cu and Zn and pore water-Cr, -Cu, and -Zn concentrations for both sediments (Fig. 5). Similarly, there were significant positive correlations between TCLP-extractable Cr and pore water Cr. These relationships indicate that environmentally relevant HMs fractions such as the C_{pw} and C_{ow} might be affected differently by human activities and non-point sources of HMs (Botté et al., 2007).

Different possible HMs immobilization mechanisms by BC can take place during the interaction period (Fig. 7). The O/C molar ratio generally denotes the content of oxygen-containing groups in BC, and the BET surface area generally represents the pore characteristics (Zhang et al., 2020). The performance of TMBC was better than either TTBC or RSBC, which might be due to its higher BET surface area and oxygen-containing groups, parameters known to influence significantly BCs adsorption capacity (Almanassra et al., 2021; Tan et al., 2015). As the increase in sediments pH in response to BC addition was non-significant, pH cannot be the main factor affecting HMs immobilization, but it can still drive other processes such as complexation, adsorption and or ion exchange. Nevertheless, the analysis of BCs mineral components (Fig. 1) indicated that the presence of oxygen reactive groups on BC surface increased BC-HMs binding capacity (Alkurdi et al., 2019; Zhang et al., 2020).

The TMBC high pH and larger surface might be the main factor affecting the reduction of the dissolved and mobile metal content, as higher pH leads to the enhancement of the net negative charge of the sediments, promoting HMs-hydroxyl binding through precipitation (Fig 7) and thereby reducing HMs solubility and bioavailability, as also mentioned by Li et al. (2020). Also, other mechanisms can be involved in HMs retention such as cation exchange, electrostatic- and/or physical adsorption, and complexation (Fig. 7), which can be driven by changes in pH. The interactions between HMs and the OH/CO functional groups on biochar surface could play a key role in the reduction of dissolved HMs, thus, reducing HMs mobility.

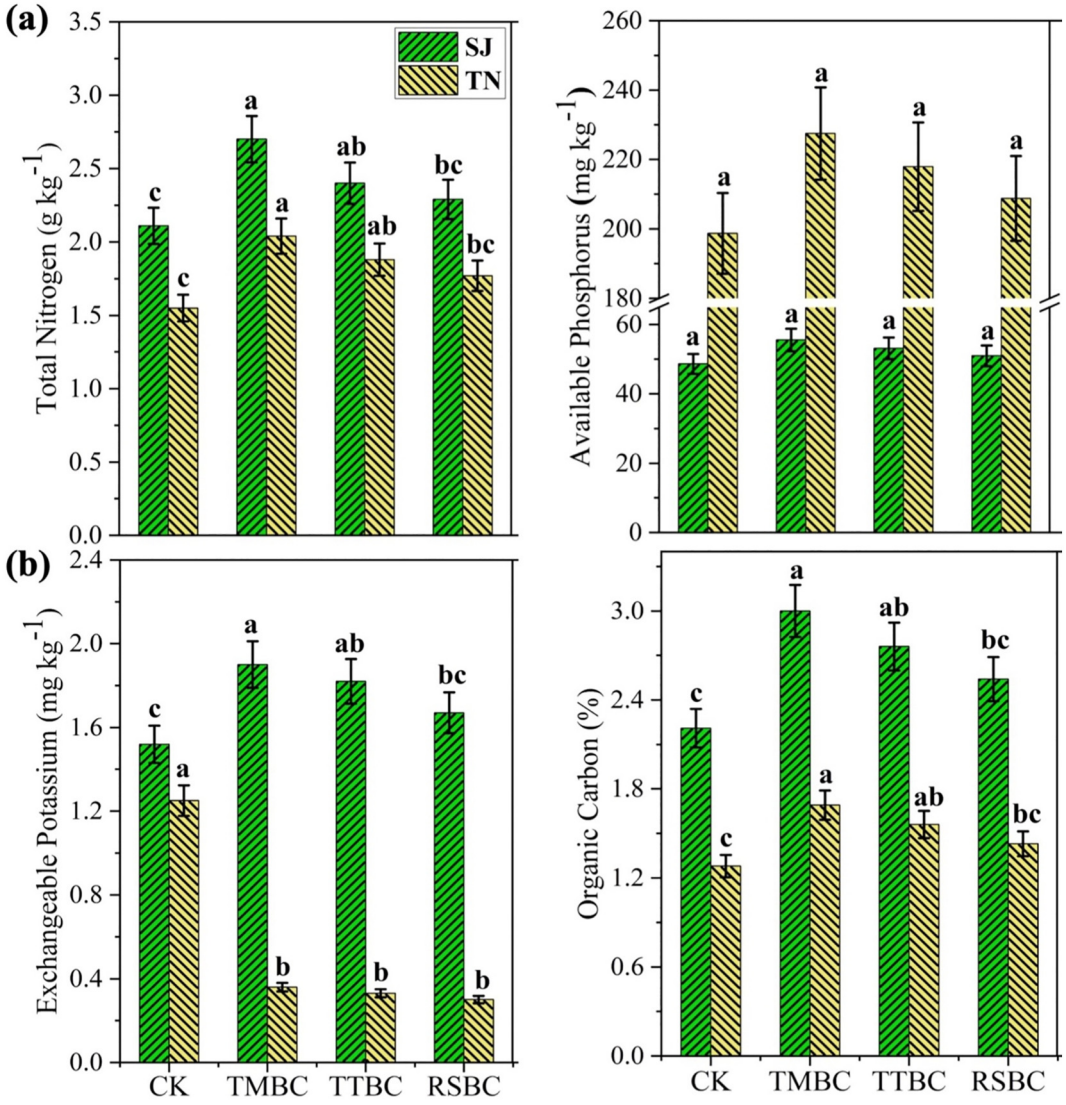

Fig. 3. Impact of biochars on the concentrations of total nitrogen (g/kg), available phosphorous (mg/kg), exchangeable potassium (mg/kg), and organic carbon (%) of the San Jiang (SJ) and Tan Niu (TN) fishpond sediments. Results are the mean values ± standard deviation (n = 3). Error bars indicate standard deviations. Different small letters on the bars indicate significant differences among treatments at $P < 0.05$.

3.5. Effect of biochars on metals fractionation

The concentration (mg/ kg) in the untreated SJ sediment of the acid-soluble fraction of was 25.2 (44% of the total content) for Cr, 3.49 (38.1%) for Cu, and 17.61 (42.8%) for Zn, whereas it was 17.3 (43.8%) for Cr, 9.3 (43.2%) for Cu, and 11.3 (45.7%) for Zn, at the TN (Table S2; Fig. 8). The acid-soluble fraction accounted for the greatest portion of the total metal content, followed by the reducible, the oxidizable, and the residual fractions (Fig. 8). The large proportion of the acid-soluble fraction and the low proportion of the residual fraction indicate the high solubility and potential mobility of these metals in both sediments, and, thus, the high potential risk.

To verify the quality of the sequential extraction results, the fractions summation of each metal was compared with the metal total content as determined by acid digestion. The results showed that the recovery percentage was rather satisfactory, ranging between 90 and 112%. These values indicate the sufficient recovery for the sequential extraction procedure, which suggests that the sequential extraction analysis allowed an acceptable quantitative recovery of total metals in the study.

The acid-soluble fraction, the most bioavailable among all fractions, of Cr, Cu, and Zn in sediments treated with the different BCs was significantly reduced compared with those in the unamended sediments (Fig. 7; Table S2). As compared with the unamended control, TMBC was more effective in reducing the average concentrations of the acid soluble Cr (by 15% in SJ and 22% in TN), Cu (by 53% in SJ and 35% in TN), and Zn (by 21% in SJ and 39% in TN) than was TTBC (by 11–15% for Cr, 30–32% for Cu, and 14–28% for Zn) or RSBC (by 10–14% for Cr, 26–27% for Cu, and 11–13% for Zn) (Fig. 8). The reducible fraction, which mainly comprises HMs bound onto Fe and Mn oxides or hydroxides, decreased with added BC concerning Cr, Cu, and Zn in both sediments, but this effect was not as well-pronounced as that observed for the acid-soluble fraction (Fig. 8).

The oxidizable metal fractions at SJ and TN were smaller than the other three fractions and slightly increased by BC addition, which might be due to the possible formation of complexes between HM ions and BCs surface reactive functional groups (Guo et al., 2006). Following the BC treatment, the residual fractions of Cr, Cu, and Zn in both sediments increased to varying degrees. Given the fact that residual HMs have almost no bioavailability, our results indicate that BC effectively increased the immobilization

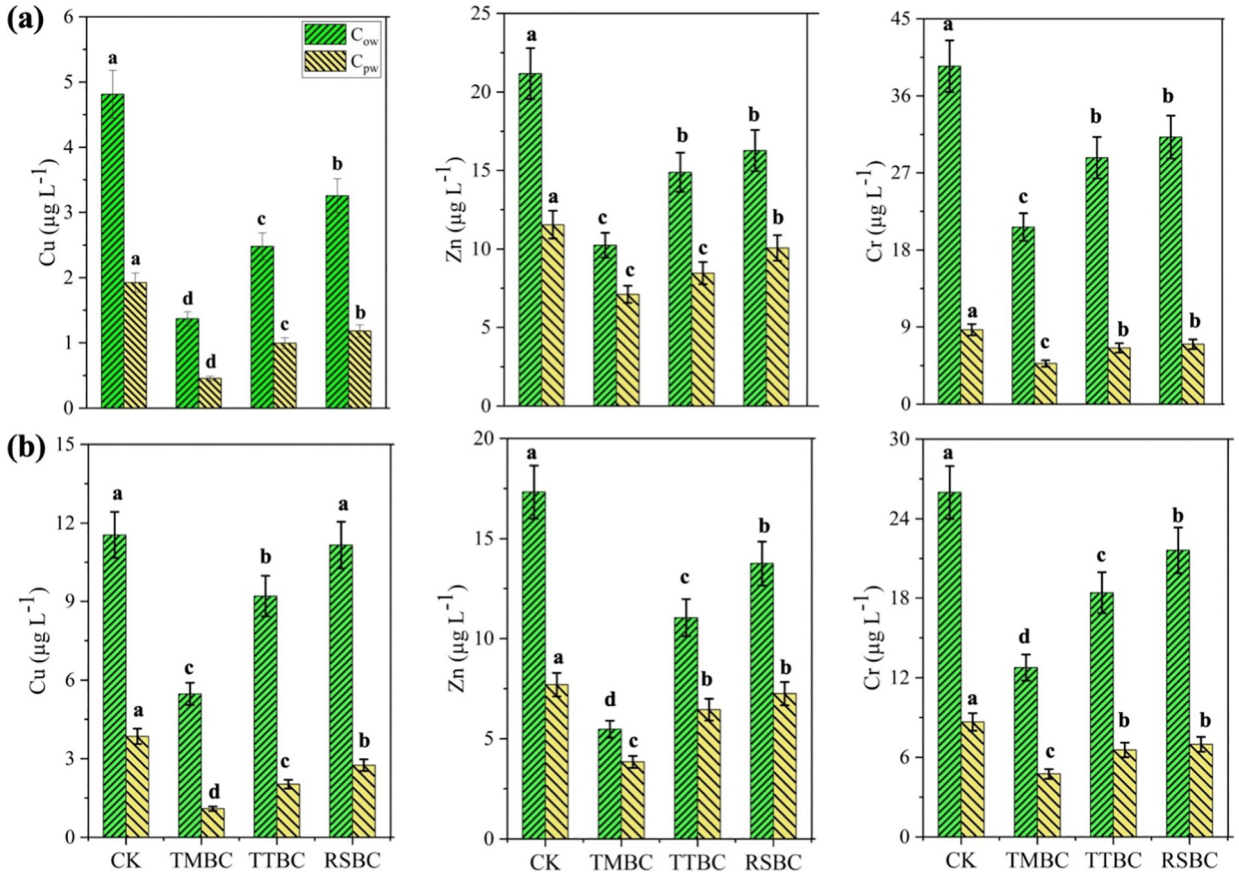

Fig. 4. Impact of biochars on the concentrations (μg L^{-1}) of Cu, Cr, and Zn in the overlying water layer (C_{ow}) and pore water (C_{pw}) of the San Jiang (SJ) fishpond sediments (a) and fish pond Tan Niu (TN) sediments (b). Results are the mean values ± standard deviation (n = 3). Error bars indicate standard deviations. Different small letters on the bars indicate significant differences among treatments at $P < 0.05$.

of HMs and promoted their transformation to more stable pools, where the degree of transformation was closely linked to the choice of BC raw materials (Fig. 8). This effect could be attributed to the substantial amounts of Ca and Mg on the BCs, which can interact with HMs to form precipitates of low solubility (Niazi et al., 2018; Ali et al., 2022); such a mechanism further immobilizes HMs in fishpond sediments, making them suitable as

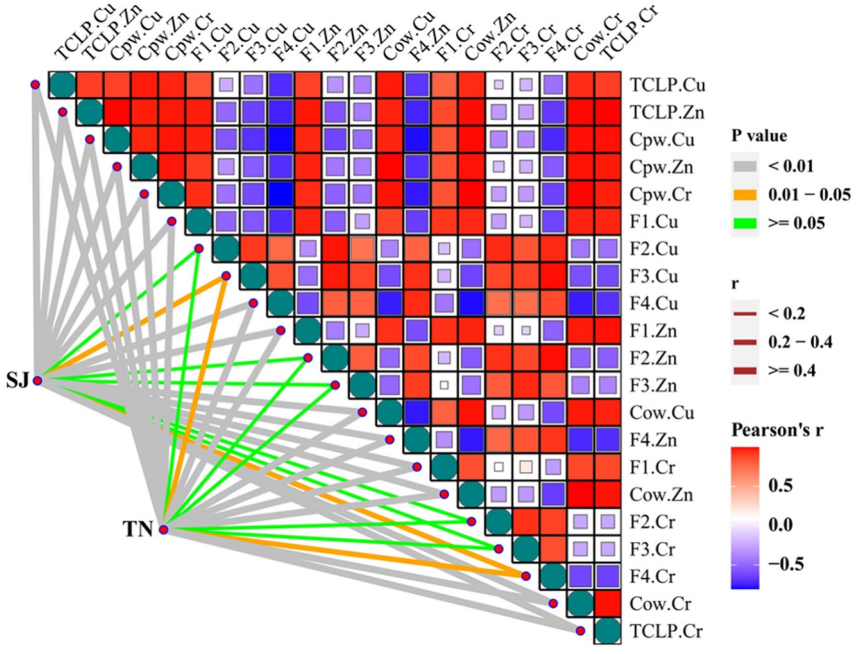

Fig. 5. Heatmap showing results of correlation coefficient and significance analysis for the effects of biochar treatment in removing heavy metals from the San Jiang (SJ) and Tan Niu (TN) fishpond sediments.

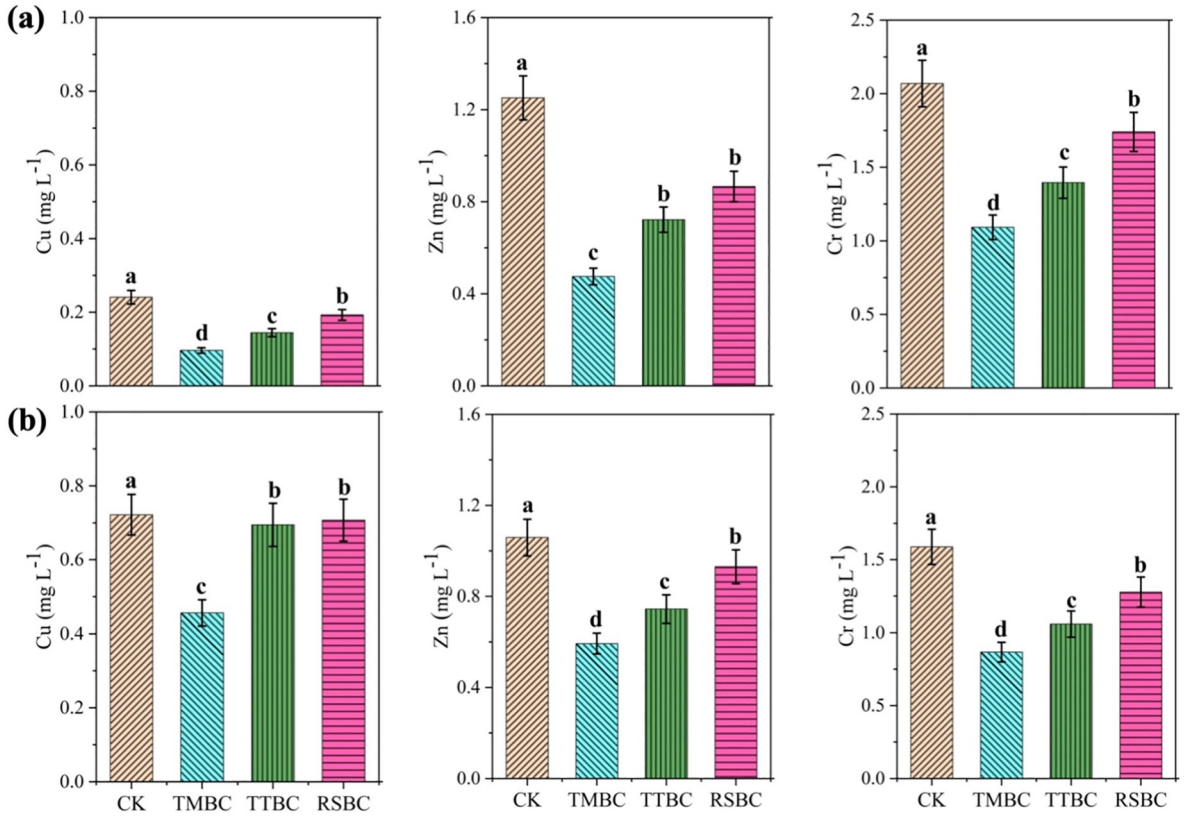

Fig. 6. Impact of biochars on the TCLP- extracted concentrations (mg L^{-1}) of Cu, Cr, and Zn in San Jiang (SJ) fishpond sediment (a) and fishpond Tan Niu (TN) sediment (b). Results are the mean values ± standard deviation (n = 3). Error bars indicate standard deviations. Different small letters on the bars indicate significant differences among treatments at $P < 0.05$.

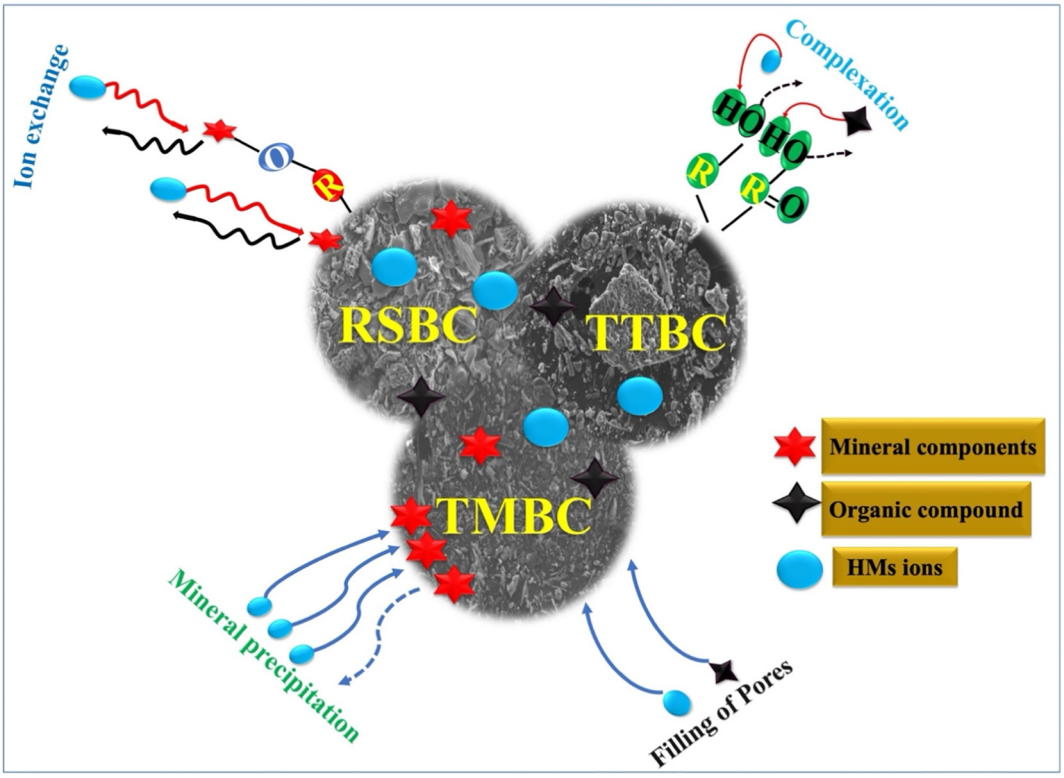

Fig. 7. Possible mechanisms of biochar action in heavy metals (HMs) immobilization in the fish pond sediments. TMCC = *Taraxacum mongolicum* Hand-Mazz-derived biochar, TTBC = *Tribulus terrestris*-derived biochar, RSBC = rice straw-derived biochar.

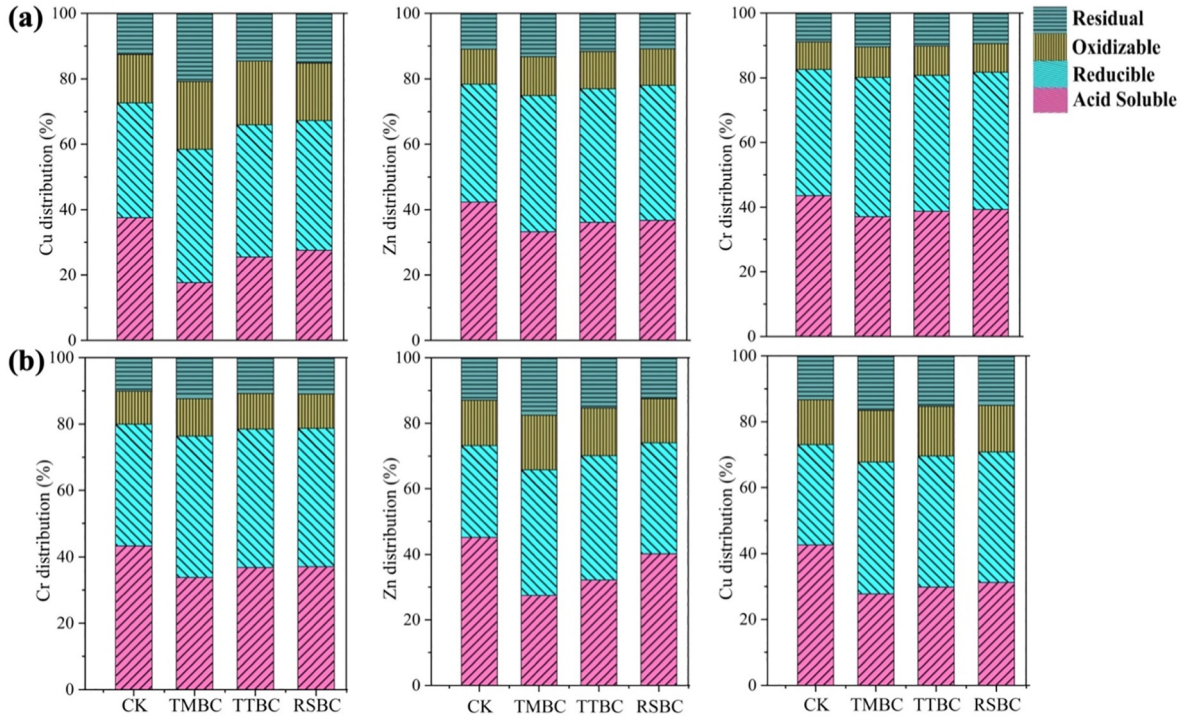

Fig. 8. Impact of biochars on the geochemical fractions of Cu, Zn, and Cr (% of total content) in the in San Jiang (SJ) fishpond sediments (a) and fishpond Tan Niu (TN) sediments (b).

amendment/fertilizers. As stated earlier, the higher active surface functional groups, higher BET surface area (Fig. 1), and higher proportion of aromatic carbon (Fig. 2) of the TMBC, compared to TTBC and RSBC, may explain the TMBC higher capacity for metal immobilization. The potential mechanisms for metals immobilization using the BCs are presented in Fig. 7.

4. Conclusions and environmental implications

This study showed that biochars (BCs) produced from *Taraxacum mongolicum* Hand-Mazz (TM), *Tribulus terrestris* (TT), and rice straw (RS) can effectively immobilize Cr, Cu, and Zn and increase the nutrient content in fishpond sediments. All tested BCs, particularly TMBC, reduced significantly the concentrations of Cr, Cu, and Zn in the overlying water and sediment pore water, and also reduced metal leachability. The TMBC reduced significantly the acid-soluble fraction of Cr, Cu and Zn, and altered these metals to their oxidizable and residual fractions and thus immobilized them in the sediments.

As the BC-sediment mixtures did not only ensure safe reduction of HM availability, but also provided a source of N and P, their application can be significantly relevant in many fields especially in low-income countries. With the current global increases in prices and demands of traditional fertilizers, BC-sediments mixture can be a significant contribution to agriculture production with multi-benefit effects including economic by allowing small-holders farmers to continue farming, environmental by ensuring the immobilization toxic metals and also for human health by ensuring safe produce free of toxic metals and safe for human and animal consumption. The use and application of the tested mixture are not only relevant for agriculture but also for public authorities, in countries with limitation in water quality and economic resources as the mixture can be tested and improved for water treatment.

The results reported here provide evidence for the selection of local raw materials for the production of BCs with high metal fixation capacity from fishpond sediments and for recycling and improving the fertilization potential of sediments. These results could be also useful for improving sediment quality when addressing its use for urban water sources protection, water quality, and water purification cost as maintaining quality water is always an important criterion for irrigation and drinking water facilities. Although the reported results are very promising, future pot and field studies and applications should validate the performance and efficiency of BC-sediment mixture in promoting agricultural production. Also, to verify the collected results under various redox conditions, further work is necessary to enlighten the processes regarding metal mobilization by the studied biochars amended fishpond sediments under controlled redox conditions combined with microscopic and spectroscopic techniques to validate the potential mechanisms for the redox mediated interactions between biochars and metals in these sediments. Moreover, more future studies are needed to examine the potential desorption of HMs from the biochar-sediment mixtures to the plants to offer a range of scientific opportunities for a comprehensive understanding of the remediation processes.

CRediT authorship contribution statement

Sajid Mehmood: Performing the experiment, data collection and treatment, creating figures, writing the draft of the manuscript.

Waqas Ahmed: Performing the experiment, investigation, analysis, and writing.

Juha Alatalo: review, editing and proof reading.

Mohsin Mahmood: Data analyses, writing, and corrections.

Muhammad Imtiaz: Review, correction, editing and proof reading.

Allah Ditta: Accurateness of data analysis, correction, and editing.

Esmat Ali:Rreview, correction, editing and proof reading.

Hamada Abdelrahman: Review, correction, editing and proof reading.

Michal Slaný: Review and editing the manuscript, particularly the data of Figs. 1 and 2.

Vasileios Antoniadis: Review, correction, editing and proof reading.

Jörg Rinklebe: Review, correction, editing and proof reading.

Sabry M. Shaheen: Writing, review, correction, editing and proof reading, and corresponding.

Weidong Li: Research idea, concept, supervision, writing, review, correction, editing and proof reading, and corresponding.

Declaration of competing interest

The authors declare that they have no known competing financial interests or personal relationships that could have appeared to influence the work reported in this paper.

Acknowledgments

We thank the National Natural Science Foundation of China for the financial support of this work (NSFC-31860728). Esmat F. Ali is thankful to Taif University Researchers Supporting Project number (TURSP-2020/65), Taif University, Saudi Arabia, for the financial support and research facilities.

Appendix A. Supplementary data

Supplementary data to this article can be found online at https://doi.org/10.1016/j.scitotenv.2022.154043.

References

Ahmed, W., Mehmood, S., Núñez-Delgado, A., Ali, S., Qaswar, M., Shakoor, A., Mahmood, M., Chen, D.Y., 2021a. Enhanced adsorption of aqueous Pb(II) by modified biochar produced through pyrolysis of watermelon seeds. Sci. Total Environ. https://doi.org/10.1016/j.scitotenv.2021.147136.

Ahmed, W., Mehmood, S., Núñez-Delgado, A., Ali, S., Qaswar, M., Shakoor, A., Maitlo, A.A., Chen, D.Y., 2021b. Adsorption of arsenic (III) from aqueous solution by a novel phosphorus-modified biochar obtained from Taraxacum mongolicum hand-mazz: adsorption behavior and mechanistic analysis. J. Environ. Manag. 292. https://doi.org/10.1016/j.jenvman.2021.112764.

Ahmed, W., Mehmood, S., Núñez-Delgado, A., Qaswar, M., Ali, S., Ying, H., Liu, Z., Mahmood, M., Chen, D.Y., 2021c. Fabrication, characterization and U(VI) sorption properties of a novel biochar derived from Tribulus terrestris via two different approaches. Sci. Total Environ. https://doi.org/10.1016/j.scitotenv.2021.146617.

Ahmed, W., Mehmood, S., Qaswar, M., Ali, S., Khan, Z.H., Ying, H., Chen, D.Y., Núñez-Delgado, A., 2021d. Oxidized biochar obtained from rice straw as adsorbent to remove uranium (VI) from aqueous solutions. J. Environ. Chem. Eng. 9. https://doi.org/10.1016/j.jece.2021.105104.

Ahmed, W., Núñez-Delgado, A., Mehmood, S., Ali, S., Qaswar, M., Shakoor, A., Chen, D.Y., 2021e. Highly efficient uranium (VI) capture from aqueous solution by means of a hydroxyapatite-biochar nanocomposite: adsorption behavior and mechanism. Environ. Res. https://doi.org/10.1016/j.envres.2021.111518.

Alamri, D.A., Al-Solaimani, S.G., Abohassan, R.A., Rinklebe, J., Shaheen, S.M., 2021. Assessment of water contamination by potentially toxic elements in mangrove lagoons of the Red Sea, Saudi Arabia. Environ. Geochem. Health 43, 4819–4830.

Ali, A., Shaheen, S.M., Guo, D., Li, Y., Xiao, R., Wahid, F., Azeem, M., Sohail, K., Zhang, T., Rinklebe, J., Li, R., Zhang, Z., 2020. Apricot shell- and apple tree-derived biochar affect the fractionation and bioavailability of zn and cd as well as the microbial activity in smelter contaminated soil. Environ. Pollut. 264, 114773. https://doi.org/10.1016/j.envpol.2020.114773.

Ali, A., Li, M., Su, J., Li, Y., Wang, Z., 2022. *Brevundimonas diminuta* isolated from mines polluted soil immobilized cadmium (Cd^{2+}) and zinc (Zn^{2+}) through calcium carbonate precipitation: microscopic and spectroscopic investigations. Sci. Total Environ. 813, 152668.

Alkurdi, S.S.A., Herath, I., Bundschuh, J., Al-Juboori, R.A., Vithanage, M., Mohan, D., 2019. Biochar versus bone char for a sustainable inorganic arsenic mitigation in water: what needs to be done in future research? Environ. Int. https://doi.org/10.1016/j.envint.2019.03.012.

Almanassra, I.W., Mckay, G., Kochkodan, V., Ali Atieh, M., Al-Ansari, T., 2021. A state of the art review on phosphate removal from water by biochars. Chem. Eng. J. https://doi.org/10.1016/j.cej.2020.128211.

Azeem, M., Shaheen, S.M., Ali, A., Jeyasundar, P.G.S.A., 2022. Removal of potentially toxic elements from contaminated soil and water using bone char compared to plant- and bone-derived biochars: a review. J. Hazard. Mater. 427, 128131.

Beiyuan, J., Lau, A.Y.T., Tsang, D.C.W., Zhang, W., Kao, C.M., Baek, K., Ok, Y.S., Li, X.D., 2018. Chelant-enhanced washing of CCA-contaminated soil: coupled with selective dissolution or soil stabilization. Sci. Total Environ. https://doi.org/10.1016/j.scitotenv.2017.09.015.

Bolan, N., Hoang, S.A., Beiyuan, J., Gupta, S., Hou, D., Karakoti, A., Joseph, S., Jung, S., Kim, K.H., Kirkham, M.B., Kua, H.W., Kumar, M., Kwon, E.E., Ok, Y.S., Perera, V., Rinklebe, J., Shaheen, S.M., Sarkar, B., Sarmah, A.K., Singh, B.P., Singh, G., Tsang, D.C.W., Vikrant, K., Vithanage, M., Vinu, A., Wang, H., Wijesekara, H., Yan, Y., Younis, S.A., Van Zwieten, L., 2022. Multifunctional applications of biochar beyond carbon storage. Int. Mater. Rev. 67 (2), 150–200. https://doi.org/10.1080/09506608.2021.1922047.

Botté, S.E., Freije, R.H., Marcovecchio, J.E., 2007. Dissolved heavy metal (Cd, pb, cr, Ni) concentrations in surface water and porewater from Bahía Blanca estuary tidal flats. Bull. Environ. Contam. Toxicol. https://doi.org/10.1007/s00128-007-9231-6.

Brewer, C.E., Chuang, V.J., Masiello, C.A., Gonnermann, H., Gao, X., Dugan, B., Driver, L.E., Panzacchi, P., Zygourakis, K., Davies, C.A., 2014. New approaches to measuring biochar density and porosity. Biomass Bioenergy https://doi.org/10.1016/j.biombioe.2014.03.059.

Chang, L., Zhao, Y., Zhang, Y., Yu, X., Li, Z., Gong, B., Liu, H., Wei, S., Wu, H., Zhang, J., 2021. Mercury species and potential leaching in sludge from coal-fired power plants. J. Hazard. Mater. 403. https://doi.org/10.1016/j.jhazmat.2020.123927.

Chen, Q., Tan, X., Liu, Y., Liu, S., Li, M., Gu, Y., Zhang, P., Ye, S., Yang, Z., Yang, Y., 2020. Biomass-derived porous graphitic carbon materials for energy and environmental applications. J. Mater. Chem. A https://doi.org/10.1039/c9ta11618d.

Cheng, Q., Wang, R., Huang, W., Wang, W., Li, X., 2015. Assessment of heavy metal contamination in the sediments from the Yellow River Wetland National Nature Reserve (the Sanmenxia section), China. Environ. Sci. Pollut. Res. 22, 8586–8593. https://doi.org/10.1007/s11356-014-4041-y.

El-Naggar, A., Shaheen, S.M., Ok, Y.S., Rinklebe, J., 2018. Biochar affects the dissolved and colloidal concentrations of cd, cu, ni, and zn and their phytoavailability and potential mobility in a mining soil under dynamic redox-conditions. Sci. Total Environ. 624, 1059–1071. https://doi.org/10.1016/j.scitotenv.2017.12.190.

El-Naggar, A., El-Naggar, A.H., Shaheen, S.M., Sarkar, B., Chang, S.X., Tsang, D.C.W., Rinklebe, J., Ok, Y.S., 2019. Biochar composition-dependent impacts on soil nutrient release, carbon mineralization, and potential environmental risk: a review. J. Environ. Manag. https://doi.org/10.1016/j.jenvman.2019.02.044.

El-Naggar, A., Shaheen, S.M., Chang, S.X., Hou, D., Ok, Y.S., Rinklebe, J., 2021. Biochar surface functionality plays a vital role in (Im)Mobilization and phytoavailability of soil vanadium. ACS Sustain. Chem. Eng. 9, 6864–6874. https://doi.org/10.1021/acssuschemeng.1c01656.

Farid, I.M., Siam, H.S., Abbas, M.H.H., Mohamed, I., 2022. Co-composted biochar derived from rice straw and sugarcane bagasse improved soil properties, carbon balance, and zucchini growth in a sandy soil: a trial for enhancing the health of low fertile arid soils. Chemosphere 292, 133389.

Fu, Q., Tan, X., Ye, S., Ma, L., Gu, Y., Zhang, P., Chen, Q., Yang, Y., Tang, Y., 2021. Mechanism analysis of heavy metal lead captured by natural-aged microplastics. Chemosphere 270. https://doi.org/10.1016/j.chemosphere.2020.128624.

Ghosh, U., Luthy, R.G., Cornelissen, G., Werner, D., Menzie, C.A., 2011. In-situ sorbent amendments: a new direction in contaminated sediment management. Environ. Sci. Technol. https://doi.org/10.1021/es102694h.

Guo, X., Zhang, S., Shan, X.Q., Luo, L., Pei, Z., Zhu, Y.G., Liu, T., Xie, Y.N., Gault, A., 2006. Characterization of pb, cu, and cd adsorption on particulate organic matter in soil. Environ. Toxicol. Chem., 2366–2373 https://doi.org/10.1897/05-636R.1.

Guo, Xia, X., Liu, Tao, H., Zhang, J., 2020. The role of biochar in organic waste composting and soil improvement: a review. Waste Manag. https://doi.org/10.1016/j.wasman.2019.12.003.

Hagemann, N., Joseph, S., Schmidt, H.P., Kammann, C.I., Harter, J., Borch, T., Young, R.B., Varga, K., Taherymoosavi, S., Elliott, K.W., McKenna, A., Albu, M., Mayrhofer, C., Obst, M., Conte, P., Dieguez-Alonso, A., Orsetti, S., Subdiaga, E., Behrens, S., Kappler, A., 2017. Organic coating on biochar explains its nutrient retention and stimulation of soil fertility. Nat. Commun. 8. https://doi.org/10.1038/s41467-017-01123-0.

Han, H., Yang, J., Ma, G., Liu, Y., Zhang, L., Chen, S., Ma, S., 2020. Effects of land-use and climate change on sediment and nutrient retention in Guizhou, China. Ecosyst. Health Sustain., 6 https://doi.org/10.1080/20964129.2020.1810592.

Haque, M.M., Belton, B., Alam, M.M., Ahmed, A.G., Alam, M.R., 2016. Reuse of fish pond sediments as fertilizer for fodder grass production in Bangladesh: potential for sustainable intensification and improved nutrition. Agric. Ecosyst. Environ. 216, 226–236. https://doi.org/10.1016/j.agee.2015.10.004.

Hossain, M.Z., Bahar, M.M., Sarkar, B., Donne, S.W., Ok, Y.S., Palansooriya, K.N., Kirkham, M.B., Chowdhury, S., Bolan, N., 2020. Biochar and its importance on nutrient dynamics in soil and plant. Biochar https://doi.org/10.1007/s42773-020-00065-z.

Jia, F., Lai, C., Chen, L., Zeng, G., Huang, D., Liu, F., Li, X., Luo, P., Wu, J., Qin, L., Zhang, C., Cheng, M., Xu, P., 2017. Spatiotemporal and species variations in prokaryotic communities associated with sediments from surface-flow constructed wetlands for treating swine wastewater. Chemosphere https://doi.org/10.1016/j.chemosphere.2017.06.132.

Jiang, J., Kou Xu, R., Yu Jiang, T., Li, Z., 2012. Immobilization of Cu(II), Pb(II) and Cd(II) by the addition of rice straw derived biochar to a simulated polluted Ultisol. J. Hazard. Mater. 229–230, 145–150. https://doi.org/10.1016/j.jhazmat.2012.05.086.

Kallenbach, R.L., McGraw, R.L., Beuselinck, P.R., 1996. Soil pH effects on growth and mineral concentration of birdsfoot trefoil. Can. J. Plant Sci. https://doi.org/10.4141/cjps96-047.

Khan, S., Naushad, M., Lima, E.C., Zhang, S.X., Shahenn, S.M., Rinklebe, J., 2021. Global soil pollution by toxic elements: current status and future perspective on the risk assessment and remediation strategies – a review. J. Hazard. Mater. 126039.

Kim, W.K., Shim, T., Kim, Y.S., Hyun, S., Ryu, C., Park, Y.K., Jung, J., 2013. Characterization of cadmium removal from aqueous solution by biochar produced from a giant miscanthus at different pyrolytic temperatures. Bioresour. Technol. 138, 266–270. https://doi.org/10.1016/j.biortech.2013.03.186.

Kong, M., Zhu, Y., Han, T., Zhang, S., Li, J., Xu, X., Chao, J., Zhang, Y., Gao, Y., 2021. Interactions of heavy metal elements across sediment-water interface in Lake jiaogang. Environ. Pollut. 286. https://doi.org/10.1016/j.envpol.2021.117578.

Kumar, M., Furumai, H., Kasuga, I., Kurisu, F., 2020. Metal partitioning and leaching vulnerability in soil, soakaway sediments, and road dust in the urban area of Japan. Chemosphere https://doi.org/10.1016/j.chemosphere.2020.126605.

Li, H., Dong, X., da Silva, E.B., de Oliveira, L.M., Chen, Y., Ma, L.Q., 2017. Mechanisms of metal sorption by biochars: biochar characteristics and modifications. Chemosphere https://doi.org/10.1016/j.chemosphere.2017.03.072.

Li, W., Zhou, J., Ding, H., Fu, H., Liu, J., Chen, Y., Dai, T., Lou, Q., Zhong, X., Fan, H., Zhong, J., 2020. Low-dose biochar added to sediment improves water quality and promotes the growth of submerged macrophytes. Sci. Total Environ. 742. https://doi.org/10.1016/j.scitotenv.2020.140602.

Liang, M., Ding, Y., Zhang, Q., Wang, D., Li, H., Lin, L., 2020. Removal of aqueous Cr(VI) by magnetic biochar derived from bagasse. Sci. Rep. 10, 21473. https://doi.org/10.1038/s41598-020-78142-3.

Lin, Y., Ye, Y., Hu, Y., Shi, H., 2019. The variation in microbial community structure under different heavy metal contamination levels in paddy soils. Ecotoxicol. Environ. Saf. https://doi.org/10.1016/j.ecoenv.2019.05.057.

Liu, P., Ptacek, C.J., Blowes, D.W., Gould, W.D., 2018. Control of mercury and methylmercury in contaminated sediments using biochars: a long-term microcosm study. Appl. Geochem. 92, 30–44. https://doi.org/10.1016/j.apgeochem.2018.02.004.

Lou, L., Luo, L., Cheng, G., Wei, Y., Mei, R., Xun, B., Xu, X., Hu, B., Chen, Y., 2012. The sorption of pentachlorophenol by aged sediment supplemented with black carbon produced from rice straw and fly ash. Bioresour. Technol. 112, 61–66. https://doi.org/10.1016/j.biortech.2012.02.058.

Miranda, L.S., Ayoko, G.A., Egodawatta, P., Hu, W.P., Ghidan, O., Goonetilleke, A., 2021. Physico-chemical properties of sediments governing the bioavailability of heavy metals in urban waterways. Sci. Total Environ. 763. https://doi.org/10.1016/j.scitotenv.2020.142984.

Mossop, K.F., Davidson, C.M., 2003. Comparison of original and modified BCR sequential extraction procedures for the fractionation of copper, iron, lead, manganese and zinc in soils and sediments. Anal. Chim. Acta 478, 111–118. https://doi.org/10.1016/S0003-2670(02)01485-X.

Niazi, N.K., Bibi, I., Shahid, M., Ok, Y.S., Burton, E.D., Wang, H., Shaheen, S.M., Rinklebe, J., Lüttge, A., 2018. Arsenic removal by perilla leaf biochar in aqueous solutions and groundwater: an integrated spectroscopic and microscopic examination. Environ. Pollut. 232, 31–41. https://doi.org/10.1016/j.envpol.2017.09.051.

Ota, Y., Suzuki, A., Yamaoka, K., Nagao, M., Tanaka, Y., Irizuki, T., Fujiwara, O., Yoshioka, K., Kawagata, S., Kawano, S., Nishimura, O., 2021. Geochemical distribution of heavy metal elements and potential ecological risk assessment of Matsushima Bay sediments during 2012–2016. Sci. Total Environ. 751. https://doi.org/10.1016/j.scitotenv.2020.141825.

Ouyang, X., Guo, F., Lee, S.Y., 2021. The impact of super-typhoon mangkhut on sediment nutrient density and fluxes in a mangrove forest in Hong Kong. Sci. Total Environ. https://doi.org/10.1016/j.scitotenv.2020.142637.

Page, A.L., 1982. Methods of Soil Analysis-Part 2: Chemical and Microbiological Properties, 2nd edition 9. Am. Soc. Agron. Inc. Publ.Madison, USA, pp. 421–422 (Phosphurus).

Palansooriya, K.N., Shaheen, S.M., Chen, S.S., Tsang, D.C.W., Hashimoto, Y., Hou, D., Bolan, N.S., Rinklebe, J., Ok, Y.S., 2020. Soil amendments for immobilization of potentially toxic elements in contaminated soils: a critical review. Environ. Int. https://doi.org/10.1016/j.envint.2019.105046.

Protection Agency (USEPA), 1991. Toxicity characteristic leaching procedure. Method 1311.

Qiu, M., Sun, K., Jin, J., Han, L., Sun, H., Zhao, Y., Xia, X., Wu, F., Xing, B., 2015. Metal/metalloid elements and polycyclic aromatic hydrocarbon in various biochars: the effect of feedstock, temperature, minerals, and properties. Environ. Pollut. 206, 298–305. https://doi.org/10.1016/j.envpol.2015.07.026.

Ramrakhian, L., Ghosh, J., Majumdar, S., 2022. Heavy metal recovery from electroplating efuent using adsorption by jute waste-derived biochar for soil amendment and plant micro-fertilize. Clean Techn. Environ. Policy https://doi.org/10.1007/s10098-021-02243-4.

Rauret, G., López-Sánchez, J.F., Sahuquillo, A., Rubio, R., Davidson, C., Ure, A., Quevaullier, Ph., 1999. Improvement of the BCR three step sequential extraction procedure prior to the certification of new sediment and soil reference materials. J. Environ. Monit. 1, 57–61.

Reguyal, F., Sarmah, A.K., 2018. Adsorption of sulfamethoxazole by magnetic biochar: effects of pH, ionic strength, natural organic matter and 17α-ethinylestradiol. Sci. Total Environ. https://doi.org/10.1016/j.scitotenv.2018.01.323.

Rinklebe, J., Shaheen, S.M., 2017. Geochemical distribution of co, cu, ni, and zn in soil profiles of fluvisols, luvisols, gleysols, and calcisols originating from Germany and Egypt. Geoderma 307, 122–138.

Rinklebe, J., Shaheen, S.M., Yu, K., 2016. Release of as, Ba, cd, cu, pb, and sr under predefinite redox conditions in different rice paddy soils originating from the U.S.A. and Asia. Geoderma 270, 21–32.

Rinklebe, J., Antoniadis, V., Shaheen, S.M., Rosche, O., Altermann, M., 2019. Health risk assessment of potentially toxic elements in soils along the Central Elbe River, Germany. Environ. Int. 126, 76–88. https://doi.org/10.1016/j.envint.2019.02.011.

Shaheen, S.M., Rinklebe, J., 2017. Sugar beet factory lime affects the mobilization of cd co, cr, cu, mo, ni, pb, and zn under dynamic redox conditions in a contaminated floodplain soil. J. Environ. Manag. 186, 253–260.

Shaheen, S.M., Rinklebe, J., Frohne, T., White, J.R., DeLaune, R.D., 2014. Biogeochemical factors governing cobalt, nickel, selenium, and vanadium dynamics in periodically flooded egyptian North Nile Delta rice soils. Soil Sci. Soc. Am. J. 78, 1065–1078.

Shaheen, S.M., Kwon, E.E., Biswas, J.K., Tack, F.M.G., Ok, Y.S., Rinklebe, J., 2017. Arsenic, chromium, molybdenum, and selenium: geochemical fractions and potential mobilization in riverine soil profiles originating from Germany and Egypt. Chemosphere 180, 553–564.

Shaheen, S.M., Niazi, N.K., Hassan, N.E., Bibi, I., et al., 2019. Wood-based biochar for the removal of potentially toxic elements in water and wastewater: a critical review. Int. Mater. Rev. 64, 216–247.

Shaheen, S.M., El-Naggar, A., Antoniadis, V., Moghanm, F.S., Zhang, Z., Tsang, D.C.W., Ok, Y.S., Rinklebe, J., 2020. Release of toxic elements in fishpond sediments under dynamic redox conditions: assessing the potential environmental risk for a safe management of fisheries systems and degraded waterlogged sediments. J. Environ. Manag. 255, 109778.

Shaheen, S.M., Antoniadis, V., Shahid, M., Yang, Y., et al., 2022a. Sustainable applications of rice feedstock in agro-environmental and construction sectors: a global perspective. Renew. Sust. Energ. Rev. 153, 111791.

Shaheen, S.M., Natasha, Mosa, A., Ali El-Naggar, A., 2022b. Manganese oxide-modified biochar: production, characterization and applications for the removal of pollutants from aqueous environments - a review. Bioresour. Technol. 346, 126581.

She, J., Wang, J., Wei, X., Zhang, Q., Xie, Z., Beiyuan, J., Xiao, E., Yang, X., Liu, J., Zhou, Y., Xiao, T., Wang, Y., Chen, N., Tsang, D.C.W., 2021. Survival strategies and dominant phylotypes of maize-rhizosphere microorganisms under metal(loid)s contamination. Sci. Total Environ. https://doi.org/10.1016/j.scitotenv.2021.145143.

Sial, T.A., Shaheen, S.M., Lan, Z., Korai, P.K., Ghani, M.I., Khan, M.N., Syed, A.-U.-A., Hussain Asghar Ali, M.N., Rajpar, I., Memon, M., Bhatti, S.M., Abdelrahman, H., Ali, E.F., Rinklebe, J., Zhang, J., 2022. Addition of walnut shells biochar to alkaline arable soil caused contradictory effects on CO_2 and N_2O emissions, nutrients availability, and enzymes activity. Chemosphere 293, 133476.

Singh, B., Singh, B.P., Cowie, A.L., 2010. Characterisation and evaluation of biochars for their application as a soil amendment. Aust. J. Soil Res., 516–525 https://doi.org/10.1071/SR10058.

Slaný, M., Jankovič, Ľ., Madejová, J., 2019. Structural characterization of organo- montmorillonites prepared from a series of primary alkylamines salts: mid-IR and near-IR study. Appl. Clay Sci. 176, 11–20. https://doi.org/10.1016/j.clay.2019.04.016.

Slaný, M., Jankovič, Ľ., Madejová, J., 2022. Near-IR study of the impact of alkyl-ammonium and -phosphonium cations on the hydration of montmorillonite. J. Mol. Struct. https://doi.org/10.1016/j.molstruc.2022.132568 Article in press.

Tan, X., Liu, Y., Zeng, G., Wang, X., Hu, X., Gu, Y., Yang, Z., 2015. Application of biochar for the removal of pollutants from aqueous solutions. Chemosphere https://doi.org/10.1016/j.chemosphere.2014.12.058.

Tang, W., Duan, S., Shan, B., Zhang, H., Zhang, W., Zhao, Y., Zhang, C., 2016. Concentrations, diffusive fluxes and toxicity of heavy metals in pore water of the Fuyang River, Haihe Basin. Ecotoxicol. Environ. Saf. 127, 80–86. https://doi.org/10.1016/j.ecoenv.2016.01.013.

Tou, F., Wu, J., Fu, J., Niu, Z., Liu, M., Yang, Y., 2021. Titanium and zinc-containing nanoparticles in estuarine sediments: occurrence and their environmental implications. Sci. Total Environ. 754. https://doi.org/10.1016/j.scitotenv.2020.142388.

Ure, A.M., 1991. Trace element speciation in soils, soil extracts and solutions. Microchim. Acta 104, 49–57.

Ure, A.M., Quevauviller, P.H., Muntau, H., Griepink, B., 1993. Speciation of heavy metals in soils and sediments: an account of the improvement and harmonization of extraction techniques undertaken under the auspices of the BCR of the commission of the European communities. Int. J. Environ. An. Ch. 51, 135–151.

Wang, X., Gu, Y., Tan, X., Liu, Y., Zhou, Y., Hu, X., Cai, X.X., Xu, W., Zhang, C., Liu, S., 2019. Functionalized biochar/clay composites for reducing the bioavailable fraction of arsenic and cadmium in river sediment. Environ. Toxicol. Chem. 38, 2337–2347. https://doi.org/10.1002/etc.4542.

Wang, J., She, J., Zhou, Y., Tsang, D.C.W., Beiyuan, J., Xiao, T., Dong, X., Chen, Y., Liu, J., Yin, M., Wang, L., 2020. Microbial insights into the biogeochemical features of thallium occurrence: a case study from polluted river sediments. Sci. Total Environ. https://doi.org/10.1016/j.scitotenv.2020.139957.

Wen, E., Yang, X., Chen, H., Shaheen, S.M., Sarkar, B., Xu, S., Song, H., Liang, Y., Rinklebe, J., Hou, D., Li, Y., Wu, F., Pohořelý, M., Wong, J.W.C., Wang, H., 2021. Iron-modified biochar and water management regime-induced changes in plant growth, enzyme activities, and phytoavailability of arsenic, cadmium and lead in a paddy soil. J. Hazard. Mater. 407. https://doi.org/10.1016/j.jhazmat.2020.124344.

Wiener, K.D., Simaika, J.P., Grenfell, S.E., Jacobs, S.M., 2020. Effects of invasive N2-fixing Acacia mearnsii on sediment nutrient concentrations in mountain streams: implications of sediment geochemistry for ecosystem recovery. Catena 195. https://doi.org/10.1016/j.catena.2020.104786.

Yaashikaa, P.R., Kumar, P.S., Varjani, S., Saravanan, A., 2020. A critical review on the biochar production techniques, characterization, stability and applications for circular bioeconomy. Biotechnol. Rep. https://doi.org/10.1016/j.btre.2020.e00570.

Yang, Y., Ye, S., Zhang, C., Zeng, G., Tan, X., Song, B., Zhang, P., Yang, H., Li, M., Chen, Q., 2021. Application of biochar for the remediation of polluted sediments. J. Hazard. Mater. https://doi.org/10.1016/j.jhazmat.2020.124052.

Zhang, W., Tan, X., Gu, Y., Liu, Shaobo, Liu, Y., Hu, X., Li, J., Zhou, Y., Liu, Sijia, He, Y., 2020. Rice waste biochars produced at different pyrolysis temperatures for arsenic and cadmium abatement and detoxification in sediment. Chemosphere 250. https://doi.org/10.1016/j.chemosphere.2020.126268.